Purification and Characterization of Enzymes Involved in the Degradation of Chemotactic *N*-Formyl Peptides†

Kiet T. Nguyen and Dehua Pei*

Department of Chemistry and Ohio State Biochemistry Program, The Ohio State University, 100 West 18th Avenue, Columbus, Ohio 43210

Received February 1, 2005; Revised Manuscript Received April 22, 2005

ABSTRACT: *N*-Formyl peptides are derived from proteolytic degradation/processing of bacterial and mitochondrial proteins and serve as potent chemoattractants for mammalian phagocytic leukocytes. A response to the chemotactic *N*-formyl peptides released by commensal bacteria in the gut region could be detrimental, leading to unwanted inflammation. Here, two enzymes that act sequentially to degrade *N*-formyl peptides were purified from the rat intestinal mucosal layer and biochemically characterized. The first enzyme cleaves chemotactic peptide f-MLF to release *N*-formylmethionine (f-Met) and dipeptide leucylphenylalanine, with a k_{cat} value of 14 s^{-1}, a K_M value of 0.60 mM, and a k_{cat}/K_M value of 22 500 M^{-1} s^{-1}. In-gel tryptic digestion followed by mass spectral fingerprinting identified the protein as the α-*N*-acylpeptide hydrolase (or acylamino acid-releasing enzyme, EC 3.4.19.1). The second enzyme hydrolyzes *N*-formylmethionine into formate and methionine with a k_{cat} value of 7.9 s^{-1}, a K_M value of 3.1 mM, and a k_{cat}/K_M value of 2550 M^{-1} s^{-1}. This protein was identified as the *N*-acylase IA (or N^{α}-acyl-L-amino acid amidohydrolase, EC 3.5.1.14). Together, these two enzymes play a protective role in degrading bacterial and mitochondrial N-formylated peptides.

All nascent polypeptides in bacteria, chloroplasts, and mitochondria contain an N-terminal formylmethionine (f-Met)[1] (*1*). In bacteria, peptide deformylase (PDF) removes the formyl group from the vast majority of nascent polypeptides (*2*). However, the deformylation process is not complete (*1*), and bacterial cells release certain small N-formylated peptides such as formyl-Met-Leu-Phe (f-MLF) into their environment (*3*, *4*). Intramitochondrially synthesized proteins typically retain their N-terminal f-Met residue, apparently due to the poor catalytic activity of mitochondrial PDF (*5*). Upon bacterial infection or tissue damage, these N-formylated peptides are released into the affected area, triggering a cascade of immunologic responses and the accumulation of leukocytes to the site of infection or injury. This process is initiated by the binding of chemotactic N-formylated peptides to the formyl-peptide receptor (FPR) located on the cell surface (*6*). FPRs belong to the seven-transmembrane domain G_i-protein-coupled receptor (GPCR) family. It has been suggested that the *N*-formyl group is a crucial determinant for ligand binding to the FPR (*7*). Since bacterial (*3*, *8*) and mitochondrial proteins (*9*) are the only sources of N-formylated peptides in nature, it has been widely accepted that these FPRs mediate the trafficking of phagocytes to sites of bacterial invasion or tissue damage (*10*). Among the chemotactic N-formylated peptides thus far discovered, f-MLF is one of the most potent.

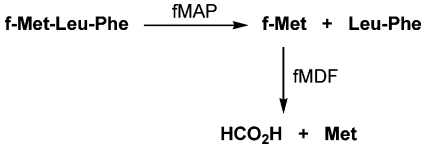

FIGURE 1: Enzymes involved in the degradation of *N*-formylmethionine peptides.

The mammalian large intestine is constantly exposed to bioactive and immunoreactive f-Met peptides, including f-MLF, released by the commensal bacteria (*11*, *12*). However, it would be detrimental if the *N*-formyl peptides should cross the intestinal mucosal barrier to provoke inflammatory responses. Indeed, colonic infusion or rectal administration of f-MLF results in experimental colitis in animals (*13*, *14*). Thus, to prevent unwanted immune response to commensal bacteria, mammals must possess enzymes that can effectively degrade the *N*-formyl peptides. Chadwick and co-workers (*15*, *16*) as well as other investigators (*17*, *18*) have previously reported that the rat intestine contains two enzymes that act sequentially to degrade the *N*-formyl peptides (Figure 1). The first enzyme, f-Met aminopeptidase (fMAP), hydrolytically removes f-Met from *N*-formyl peptides including f-MLF, eliminating their chemotactic activities. Subsequently, f-Met deformylase (fMDF) further converts f-Met into formate and methionine (*16*−*18*). It was reported that fMAP is specific for *N*-formylmethionyl and *N*-acylmethionyl peptides and has no activity toward other N-acylated amino acids (e.g., f-Ala, f-Val, f-Leu, f-Arg, and

† This work was supported by a grant from the National Institutes of Health (AI40575).

* To whom all correspondence should be addressed at Dehua Pei, Department of Chemistry, The Ohio State University, 100 West 18th Avenue, Columbus, OH 43210. Phone, 614-688-4068; fax, 614-292-1532; e-mail, pei.3@osu.edu.

[1] Abbreviations: f-MLP, *N*-formyl-methionyl-leucyl-phenylalanine; f-Met, *N*-formyl-methionine; Ac-Met, *N*-acetyl-methionine; f-M-*p*NA, *N*-formyl-methionyl-*para*-nitroanilide; FDH, formate dehydrogenase; HEPES, *N*-2-hydroxyethylpiperazine-*N*′-2-ethanesulfonic acid; DEPC, diethylpyrocarbonate; Tris, tris (hydroxymethyl) aminomethane; fMAP, *N*-formylmethionine aminopeptidase; fMDF, *N*-formylmethionine deformylase; APH, α-*N*-acylpeptide hydrolase; FCR, formyl-peptide receptor; PDF, peptide deformylase.

10.1021/bi050191o CCC: $30.25
Published on Web 05/19/2005

f-Phe derivatives) (*15*). Although the enzyme was purified to near homogeneity, its identity has not yet been established. Other investigators have purified enzymes with α-*N*-acylpeptide hydrolase (APH or acylamino acid-releasing enzyme, EC 3.4.19.1) activities from sheep (*19*), rabbit (*20*), and human erythrocytes (*21*), rat liver (*22*−*24*), and rabbit skeletal muscle (*25*), which are capable of releasing f-Met from *N*-formylmethionyl peptides. However, the latter enzymes seem to have different substrate specificity profiles from fMAP (*15*). The identity of fMDF also remains to be determined. In accordance with Chadwick and co-workers (*16*), fMDF is most active against f-Met and *N*-formylnorleucine, has reduced activity against f-Leu, but is inactive against other *N*-formyl amino acids or *N*-formylmethionyl peptides. fMDF activities have also been described in crude extracts of rabbit reticulocytes (*20*), human leukocytes, and platelets (*17*) and *Euglena gracilis* (*18*). Again, in neither case has the identity of the enzyme been established.

We have undertaken the purification and characterization of fMAP and fMDF to understand their roles in the degradation of *N*-formyl peptide chemotactic agents. Our interest stems from our ongoing work on bacterial PDF, which is currently being pursued as a novel antibacterial drug target (*2*). However, treatment of bacteria cells with PDF inhibitors may result in the accumulation of *N*-formyl peptides (*26*), a condition that could potentially induce unwanted inflammatory responses. In this work, we have purified both fMAP and fMDF to homogeneity and established their identities as APH and *N*-acylase IA, respectively. Detailed characterization of their substrate specificities suggests that they are responsible for the degradation of *N*-formyl peptides.

EXPERIMENTAL PROCEDURES

Materials. Small intestines from Sprague−Dawley rats were purchased from Zivic Laboratories (Pittsburgh, PA). NAD^+, Triton X-100, and *Candida boidinii* formate dehydrogenase (FDH) were purchased from Sigma. f-MLF, fluorescamine, *p*-nitroaniline, 1,10-phenanthroline, and diethyl pyrocarbonate were purchased from Aldrich. f-Met, Ac-Met, and other peptide derivatives were purchased from Bachem Biosciences, Inc. Reagents for peptide synthesis were purchased from Advanced ChemTech (Louisville, KY). N^{ϵ}-Formyl-N^{ϵ}-hydroxy-L-lysine was chemically synthesized by Dr. G. Shen of this laboratory, and the synthesis details will be reported elsewhere.

Buffers. Buffers used were the following: buffer A, 150 mM NaCl and 30 mM Tris, pH 7.5; buffer B, 20 mM Tris and 10 mM NaCl, pH 8.0; buffer C, 1.7 M $(NH_4)_2SO_4$ and 100 mM KH_2PO_4, pH 7.0; buffer D, 100 mM KH_2PO_4, pH 7.2; buffer E, 50 mM Tris and 75 mM NaCl, pH 7.5; buffer F, 150 NaCl and 50 mM HEPES, pH 7.0; buffer G, 200 mM KCl and 200 mM sodium borate, pH 9.0; buffer H, 10 mM sodium phosphate and 0.5 M NaCl, pH 7.5; buffer I, 20 mM sodium phosphate, pH 7.4; and buffer J, 50 mM sodium acetate, pH 5.5.

Synthesis of N-Formyl-methionyl-p-nitroaniline (f-M-pNA). Fmoc-methionine and *p*-nitroaniline were thoroughly dried over phosphorus pentoxide. Fmoc-methionine (2.0 mmol) and *p*-nitroaniline (2.0 mmol) were dissolved in 8 mL of dry pyridine. The mixture was brought to −20 °C in a methanol/dry ice bath. Trichlorophosphorus oxide (3.2 mmol) was slowly added to the chilled solution, and the reaction was allowed to proceed for 2 h. The reaction was brought to room temperature and stirred for 3 h. The reaction was neutralized with 50 mL of 5% sodium bicarbonate, extracted with ethyl acetate (3 × 15 mL), and washed with 0.5 M HCl (3 × 30 mL). The solvent was evaporated under reduced pressure to give 389 mg product (40% yield). The Fmoc group was removed by dissolving the solid in 5 mL of 20% piperidine in dichloromethane for 1 h at room temperature. The product was recrystallized from methanol. The resulting methionyl-*p*-nitroanilide was N-formylated by treatment with 3 mL of 96% formic acid and 1 mL of acetic anhydride at 0 °C. The reaction product was purified by flash column chromatography (silica gel) to give 100 mg of a white solid. ^{1}H NMR (250 MHz, $CDCl_3$) δ 9.18 (s, 1H), 8.30 (s, 1H), 8.23−7.68 (m, 4H), 6.53 (d, J = 7.5 Hz, 1H), 4.93 (m, 1H), 2.67 (m, 2H), 2.27 (m, 2H), 2.15 (s, 3H). ESI−HRMS: calcd for $C_{12}H_{15}N_3O_4SNa^+$ ($M + Na^+$): 320.0675. Found: 320.0672.

Purification of fMAP. Fifteen frozen rat small intestines (−80 °C) were thawed and washed with ice-chilled buffer A. The loosely bound mucosal layer was removed by gently scraping the inside lining of the small intestines, washed with buffer A (3 × 100 mL), and centrifuged at 4 °C for 10 min at 500*g* (Sorvall GS-3 rotor). The pellet was resuspended in 30 mL of buffer A and sonicated for 5 × 10 s pulses (medium probe, Branson). The suspension was adjusted to 10 mM $CaCl_2$, stirred at 4 °C for 30 min, and centrifuged at 4 °C for 90 min at 200 000*g* (Beckman Ti-70 rotor). The solution (35 mL) was diluted with ice-chilled ddH_2O (final volume 150 mL) and loaded onto a Q-Sepharose Fast Flow (Pharmacia) column (2.5 cm × 12 cm) preequilibrated in buffer B. The adsorbed proteins were eluted with 300 mL of buffer B and a linear gradient of 10−500 mM NaCl. Fractions that showed activity toward f-M-*p*NA and f-MLF substrates were pooled (Figure 2A) and concentrated to 37 mL in an Amicon YM-10 nitrocellulose concentrator. The solution was adjusted to 1.7 M ammonium sulfate (final concentration) and loaded onto a Pharmacia Phenyl-Sepharose column (1.6 cm × 10 cm) preequilibrated in butter C. Elution was performed with buffer C and a reverse ammonium sulfate linear gradient with buffer D (1.7−0 M; 300 mL at 2.0 mL/min). Active fractions (Figure 2B) were pooled and loaded onto a Pharmacia FPLC Mono Q column (HR 5/5) preequilibrated in buffer B. Elution was performed with a linear gradient of 10 mM−1.0 M NaCl over 20 mL. Active fractions were pooled and precipitated with 85% ammonium sulfate and centrifuged for 30 min at 4 °C (30 000*g*). The pellet was dissolved in 500 μL of buffer E and passed through a Superdex S-200 column (1.0 cm × 30 cm) equilibrated in buffer E at a flow rate of 0.5 mL/min. The active fractions were pooled and concentrated with a Millipore YM-10 filter. The protein concentration was determined by the Bradford assay using bovine serum albumin as the protein standard.

Purification of fMDF. Twenty frozen rat small intestines (−80 °C) were thawed and washed with buffer H. The fecal matter was discarded, and the mucosal layer was removed from the intestinal lining. The suspension was washed with 200 mL of buffer I with centrifugation at 500*g* and 4 °C (Sorvall GS-3 rotor). The loosely packed pellet was resuspended in 150 mL of buffer I and sonicated for 5 × 10 s pulses (medium probe, Branson). The reddish suspension was

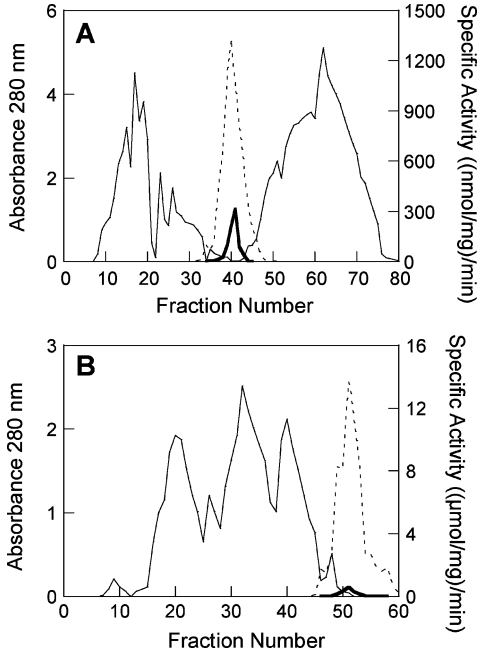

FIGURE 2: Chromatograms for the purification of fMAP. (A) Fractionation on a Q-Sepharose column. (B) Fractionation on a phenyl-Sepharose column. Solid line, protein concentration as monitored by their absorbance at 280 nm; dashed line, specific activity of fMAP as determined with f-M-*p*NA as substrate; and bold line, specific activity of fMAP as determined with f-MLF as substrate.

centrifuged at 27 000*g* (Sorvall SS-34 rotor) for 60 min at 4 °C. The supernatant was diluted with ice-cold water to a final volume of 200 mL. The pH of the solution was adjusted to 5.5 with ice-chilled (1/5 dilution) glacial acetic acid, and centrifugation was continued for 15 min. The solution was loaded onto a CM-Sepharose column (2.5 cm × 10 cm, Sigma) preequilibrated in buffer J. fMDF activity appeared in the flow-through fractions. The flow-through fractions were loaded onto an SP-Sepharose column (2.5 cm × 10 cm, Pharmacia) preequilibrated in 25 mM Mes, pH 6.0, to remove additional proteins. The pH of the flow-through fractions was readjusted to 8.0 with a 1.5 M Tris (pH 8.0) solution. The mixture was loaded onto a Q-Sepharose column (2.5 cm × 16 cm, Pharmacia) preequilibrated in buffer B. The adsorbed proteins were eluted with 300 mL of buffer B plus a linear gradient of 10−500 mM NaCl. Fractions containing activity against f-Met were pooled, brought to a concentration of 25% ammonium sulfate, and loaded onto an octyl-Sepharose column (2.5 cm × 8 cm, Pharmacia) preequilibrated in buffer D. The strongly adsorbed protein was washed with 200 mL of buffer D and eluted with 150 mL of the same buffer and a linear gradient of 0−4% Triton X-100. Fractions with fMDF activity were pooled and loaded onto a Mono-Q column (HR 5/5, Pharmacia) preequilibrated in buffer B. Elution of the adsorbed protein was effected with 20 mL of buffer B and a linear gradient of 10−500 mM NaCl. The active fractions were pooled and passed through a Superdex S-200 gel filtration column (1.0 cm × 30 cm, Pharmacia) preequilibrated in buffer E. Protein solution was passed through a small Concanavalin A-Sepharose column (1 g). Active fMDF fractions were pooled and concentrated with a Millipore YM-10 nitrocellulose filter and stored at −80 °C. The protein concentration was determined by the Bradford assay using bovine serum albumin as the protein standard.

Metal Analysis. Prior to experiments, all tubes and plastic containers were soaked overnight with 2% nitric acid solution, washed with 6 g/L EDTA solution, and rinsed three times with ultrapure water prepared from a Barnstead E-pure system at 18.3 MΩ. Protein samples were diluted in a solution containing 1 g/L ammonium dihydrogen phosphate and 1% (v/v) HNO_3. The metal content of fMDF was analyzed on a Perkin-Elmer Zeeman 5000 graphite furnace atomic absorption spectrometer equipped with an AS40 autosampler (20 μL-injection samples). The presence of Zn was detected with a zinc lamp at 213.9 nm. A standard curve was generated using known concentrations of zinc chloride.

To confirm the zinc content from atomic absorption experiments, a direct colorimetric assay was also carried out by using 2-(5-nitro-2-pyridylazo)-5-(*N*-propyl-*N*-sulfopropylamino)phenol disodium salt dehydrate (nitro-PAPS) (*27*). The reactions were carried out in 100 μL total volume containing 90 μM nitro-PAPS, 6.0 M guanidine hydrochloride, and 200 mM Tris·HCl, pH 8.1, and 0−10 μg of fMDF. The absorbance at 572 nm was measured on a Perkin-Elmer Lambda 25 UV/vis spectrophotometer. A standard curve was generated similarly by using known concentrations of $ZnSO_4$.

fMAP Assay. fMAP activity was assayed by two different methods. In method A, assay reactions were performed in polystyrene cuvettes (1 mL total volume) containing buffer F and 0−800 μM f-M-*p*NA. The reaction was initiated by the addition of 0.56 μg of fMAP and continuously monitored at 405 nm on a Perkin-Elmer Lambda 25 UV/vis spectrophotometer. Method B employs *N*-formyl peptides (0−20 mM) as substrates. Reactions (100 μL total volume in buffer F) were initiated by the addition of 0.56 μg of fMAP and incubated at room temperature for 15 min. The reaction was quenched by heating at 100 °C for 30 min and centrifuged to remove the precipitated proteins. The solution was diluted to 200 μL in ddH_2O, and 200 μL of buffer G was added. To determine the amount of free amine formed, 200 μL of a fluorescamine solution (0.1 mg/mL in ethanol) was added and the fluorescence yield was measured on an Aminco-Bowman Series 2 Luminescence spectrometer (excitation wavelength at 390 nm and emission wavelength at 475 nm). The amount of product formed was determined by comparison to a standard line generated with methionine. Inhibition of fMAP was carried out in a total volume of 1 mL containing 150 mM NaCl and 50 mM HEPES, pH 7.0, 0.39 mM f-M-*p*NA, and various concentrations of an effector molecule (e.g., 1,10-phenanthroline). The reaction was initiated by the addition of 0.56 μg of fMAP, and the absorbance at 405 nm was monitored for 60 s. fMAP reactions were also carried out in buffers of various pH values to assess the effect of pH on the catalytic activity. The buffers used were 50 mM NaOAc for pH 5.0−5.5, 50 mM Mes for pH 6.0−6.5, 50 mM HEPES for pH 7.0−7.5, 50 mM Tris·HCl for pH 8.0−8.5, 50 mM CHES for pH 9.0−9.5, and 50 mM $NaHCO_3$ for pH 10.0. Reactions were carried out in 500 μL total volume containing the indicated buffers, 0.56 μg fMAP, and 800 μM f-M-*p*NA. Product formation was monitored continuously at 405 nm on a Perkin-Elmer Lambda 25 UV/vis spectrophotometer.

fMDF Assay. Two methods were employed to assay fMDF activity. In method A, the amount of formate released was quantitated by using formate dehydrogenase (FDH) as the coupling enzyme. The reaction (500 μL total volume)

contained buffer F, 5 mM NAD^+, 1.0 unit FDH, and 0−10 mM f-Met as substrate. The reaction was initiated by the addition of fMDF (final concentration 24 nM) and monitored continuously at 344 nm on a Lambda 25 UV/vis spectrophotometer. In method B, assay reactions were performed in 200 μL of buffer F containing 0−3.0 mM *N*-acetyl-L-methionine. The reaction was initiated by the addition of fMDF (final concentration 24 nM) and allowed to proceed for 5 min at room temperature. The reaction was quenched by the addition of 10 μL of trichloroacetic acid and centrifuged at 14 000 rpm in a microcentrifuge for 10 min. The pH of the supernatant was adjusted by the addition of 200 μL of buffer G. Product formation was analyzed by the addition of 200 μL of 0.1 mg/mL fluorescamine solution, and the fluorescence yields were measured immediately as described above. In addition, fMDF assays were carried out in buffers of various pH values to assess the effect of pH on the catalytic activity. The buffers used were 50 mM NaOAc for pH 4.0−5.5, 50 mM Mes for pH 6.0−6.5, 50 mM HEPES for pH 7.0−7.5, 50 mM Tris·HCl for pH 8.0−8.5, 50 mM CHES for pH 9.0−9.5, and 50 mM $NaHCO_3$ for pH 10.0. The pH profile analysis was carried out using method B and 10 mM f-Met as substrate.

Gel-Filtration Analysis. Analysis was performed on a Superdex S-200 column (Pharmacia, 10/30 GL) connected to an AKTA/*FPLC* (Amersham) at flow rate of 0.5 mL/min. The column was preequilibrated in buffer A. Protein samples (200 μL) were injected onto the FPLC column, and elution was monitored at 280 nm wavelength. Protein molecular weight standards were ovalbumin (45 kDa), albumin (66 kDa), aldolase (158 kDa), catalase (232 kDa), and ferritin (440 kDa).

In-Gel Digestion. Protein samples were separated on 12% SDS−PAGE gels under reducing conditions. Gels were fixed overnight in a 50:10:40 ethanol/acetic acid/water solution and stained with Coomassie blue G-250. The desired protein band was excised and washed with the ethanol/acetic acid/water solution for several hours. The gel slice was dried with acetonitrile and treated with a dithiothreitol solution to reduce any disulfides. Iodoacetamide was added to alkylate the cysteines, and the gel was washed with cycles of acetonitrile and ammonium bicarbonate solution. The resulting gel slice was treated overnight at room temperature with sequencing grade trypsin (Promega, Madison, WI) by using the Montage In-Gel Digestion Kit (Millipore, Bedford, MA) and following manufacturer's recommended protocols. The peptides were extracted from the polyacrylamide gel with a 50:5:45 acetonitrile/formic acid/water solution several times, pooled, and concentrated in vacuo to ~25 μL.

Nano-LC MS/MS. This method was employed to identify tryptic digested fMDF peptides. Capillary-liquid chromatography-nanospray tandem mass spectrometry (Nano-LC MS/MS) was performed on a Micromass hybrid quadrupole time-of-flight Q-Tof II (Micromass, Wythenshawe, U.K.) mass spectrometer equipped with an orthogonal nanospray source from New Objective, Inc. (Woburn, MA) operated in positive ion mode. The LC system was a LC-Packings-Dionex Capl LC. Solvent A was water containing 50 mM acetic acid, and solvent B was acetonitrile. Each sample (2.5 μL) was first injected into the trapping column and washed with 50 mM acetic acid. The injector port was switched to the "inject" position, and the peptides were eluted off the trap onto the LC column. A ProteoPep C18 column (5 cm × 75 μm) packed directly in the nanospray tip was used for chromatographic separations. Peptides were eluted directly off the column into the Q-Tof system using a gradient of 2−80% of solvent B over 30 min, at a flow rate of 40 μL/min with a precolumn split to about 500 nL/min. The total running time was 55 min. The nanospray capillary voltage was set at 3.0 kV and the cone voltage at 55 V. The source temperature was maintained at 100 °C. Mass spectra were recorded using MassLynx 4.0 with automatic switching functions. Mass spectra were acquired from mass 400−2000 Da every 1 s with a resolution of 8000 (fwhm). When a desired peak was detected at a minimum of 15 ion counts, the mass spectrometer was automatically switched to acquire CID MS/MS spectrum of the individual peptide. Collision energy was set dependent on charge state recognition properties. Sequence information from the MS/MS data was processed using Mascot Distiller. Database searches were performed using Mascot and Genomic Solutions.

Table 1: Purification of fMAP from Rat Epithelial Mucosal Layer

purification step	total protein (mg)	specific activity[a] ((nmol/min)/mg protein)	purification (fold)	recovery (%)
crude sonicate	1940	8.0	1	100
anion exchange	320	240	29	67
phenyl-Sepharose	3.0	3140	374	43
Mono Q	1.2	8550	1018	33
gel filtration	0.7	17300	2061	20

[a] The substrate for the purification and activity assay was f-Met-*p*-NA.

RESULTS

Purification of fMAP and fMDF. fMAP was purified in a similar manner as described by Chadwick et al. (Table 1) (*15*). Upon removal of loosely bound mucosal layer from the small intestine, sonication, and centrifugation at 200 000*g* to remove organelles and brush-border membrane vesicles, the enzyme activity remained in the supernatant fraction. During purification, fMAP activity was initially monitored by assay method A, which employs f-M-*p*NA as substrate and is very sensitive and convenient. Throughout the purification procedure, we were able to detect only a single fraction that is capable of cleaving f-M-*p*NA to release *p*-nitroaniline (Figure 2). To ascertain that this fraction contained the fMAP activity, all fractions were subsequently assayed against f-MLF (assay method B). The same activity profile was obtained. A combination of anionic exchange (Q-Sepharose and Mono Q), hydrophobic interaction (phenyl-Sepharose), and gel-filtration chromatographic steps resulted in a 2061-fold purification of the enzyme. The purified protein showed one major band at $M_r \sim 66\,000$ Da on SDS−PAGE gels (Figure 3A). Gel-filtration analysis of the protein gave a native molecular mass of ~280 000 Da. As reported previously (*15*), the enzyme did not bind to either wheat germ agglutinin or concanavalin A-Sepharose, indicating that the enzyme is not glycosylated. These results suggest that the native fMAP is a homotetramer.

Purification of fMDF from the small intestinal epithelial mucosal layer also followed a literature procedure (*16*) but with a number of modifications (Table 2). After cell lysis and centrifugation (200 000*g*), fMDF activity remained in

Table 2: Purification of fMDF from Rat Epithelial Mucosal Layer

purification step	total protein (mg)	specific activity[a] ((nmol/min)/ mg protein)	purification (fold)	recovery (%)
crude lysate	2210	1.2	1	100
acidification	575	1.9	2	90
CM-Sepharose	112	3.9	3	85
Q-Sepharose	45	89	74	56
octyl-Sepharose	5.0	320	267	40
size exclusion	0.5	1900	1583	32
concanavalin A-Sepharose	0.3	2200	1833	26

[a] The substrate for the purification and activity assay was f-Met.

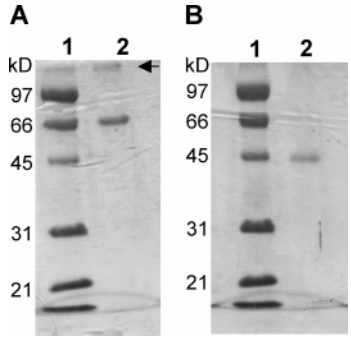

FIGURE 3: Coomassie Blue-stained SDS−PAGE gels (10%) showing the purified fMAP (A) and fMDF (B). Lane 1, molecular weight markers, and lane 2, purified fMAP or fMDF. The bands indicated by the arrow are due to some proteins retained in the sample loading wells.

the supernatant fraction. The enzyme was stable after acidification of the supernatant to pH 5.5. This greatly facilitated its purification, as many proteins precipitated at this pH and were readily removed by centrifugation. The deformylase was also apparently very hydrophobic, binding exceptionally tightly to an octyl-Sepharose column. Triton X-100 detergent was required to elute the protein off the column. Overall, fMDF was purified 1833-fold by a combination of acidification, two anion-exchange chromatographic steps, a hydrophobic interaction step, a size exclusion step, and an affinity chromatographic step. The purified enzyme showed a molecular mass of ~45 000 Da in both SDS−PAGE and gel-filtration analyses, indicating that fMDF exists as a monomer in the purified form (Figure 3B).

Identification of fMAP and fMDF by Mass Spectrometry. Protein bands corresponding to fMAP and fMDF were excised from SDS−PAGE gels and digested to completion with trypsin, and the resulting peptides were analyzed by LC-ESI mass spectrometry. The obtained peptide masses were then used to search against the NCBI database for potential matches. Such analysis of fMAP resulted in a single match with APH from rat liver with a score of 112. Out of a total of 27 peptide fragments derived from the fMAP sample, 19 matched exactly the calculated masses of the corresponding peptides in APH (Table 3). However, rat APH contains 732 amino acid residues and has a calculated molecular mass of 81 347 Da (*28*), which is significantly larger than the observed fMAP molecular mass of ~66 kDa (Figure 3A). We noted that all 19 matched peptides in Table 3 are located in the C-terminal region of APH, with the first peptide (YCTNR) matching the amino acids 274−278 of APH. This suggests that the purified fMAP is a proteolytic fragment of APH (C-terminal fragment). The proteolysis may have occurred in animals as a physiological process or during the lengthy purification procedure. It is also possible that fMAP is a splicing variant of the full-length APH. Like fMAP, native APH also exists as a homotetramer of 340 000 Da (*28*).

Table 3: Identification of fMAP by MS Analysis of Tryptic Fragments

peptide[a]	observed ($M + H^+$)	M_r (calcd)	M_r (expt)
N^{691}VPRV^{695}	584.49	583.34	583.48
R^{674}VPFK^{678}	646.55	645.40	645.54
$Y^{274}C^{b}$TNR^{278}	713.47	712.30	712.46
$Y^{274}C^{b}$TNRR^{279}	869.62	868.40	868.61
L^{307}SPDQ$C^{b}R^{313}$	875.63	874.40	874.62
V^{435}GFLPPPGK^{443}	911.70	910.53	910.69
V^{376}VFDSAQR^{383}	921.72	920.47	920.71
Q^{682}GMEYYR^{688}	946.65	945.40	945.65
Q^{682}GM^{c}EYYR^{688}	962.65	961.40	961.64
V^{340}TSVVVDIVPR^{350}	1183.97	1182.70	1182.96
M^{528}GFAVLLVNYR^{538}	1282.99	1281.69	1281.98
T^{665}PVLLMLGQEDR^{676}	1372.03	1370.72	1371.03
T^{665}PVLLM^{c}LGQEDR^{676}	1388.00	1386.72	1386.99
T^{665}PVLLMLGQEDRR^{677}	1528.15	1526.82	1527.15
$C^{292(c)}$ELLSDGSLAIC^{c}SPR^{306}	1678.16	1677.79	1677.16
D^{562}VQFAVEQVLQEEHFDAR^{579}	2160.41	2159.03	2159.41
G^{539}STGFGQDSILSLPGNVGHQDVK^{561}	2313.53	2312.14	2312.53
E^{444}QSVSQVSLEEAEPIPGIHWGVR^{466}	2605.68	2604.30	2604.67
Q^{351}LGESFSGIYC^{c}SLLPLGC^{c}WSADSQR^{375}	2831.67	2830.31	2830.66

[a] Peptide fragments shown correlate to indicated regions within the *N*-acylaminopeptidase polypeptide. [b] Carbamidomethyl cysteine. [c] Oxidation of methionine.

Table 4: Identification of FMDF by MS/MS Analysis of Tryptic Fragments

peptide[a]	observed	M_r (expt)	M_r (calc)
R^{161}PEFQALR^{168}	508.94	1015.87	1015.56
V^{222}VNSILAFR^{230}	509.97	1017.93	1017.60
E^{245}GAVTSVNLTK^{255}	559.99	1117.96	1117.60
S^{116}VSIQYLEAVR^{126}	633.05	1264.08	1263.68
L^{393}VAALASVPALPGES^{408}	698.12	1394.23	1393.78
A^{354}VGIPALFGSPMNR^{367}	715.61	1429.21	1428.75
A^{354}VGIPALGFSPM^{b}NR^{367}	723.62	1445.23	1444.75

[a] Peptide fragments shown correlate to indicated regions within the N-acylase I polypeptide. [b] Oxidation of Methionine.

Analysis of fMDF peptides was performed in a slightly different manner. The peptides derived from a tryptic digest of fMDF were analyzed by electrospray-ionization tandem mass spectrometry (ESI-MS/MS). The individual peptides were fragmented in the second spectrometer by collision-induced dissociation (CID), and the resulting product ions were analyzed with Mascot software. Out of a total of 12 peptides examined, 7 matched exactly with peptide fragments from N-acylase IA with a score of 254 (Table 4). The next two potential matches were a trypsin precursor and a putative calcium binding protein, with scores of 49 and 36, respec-

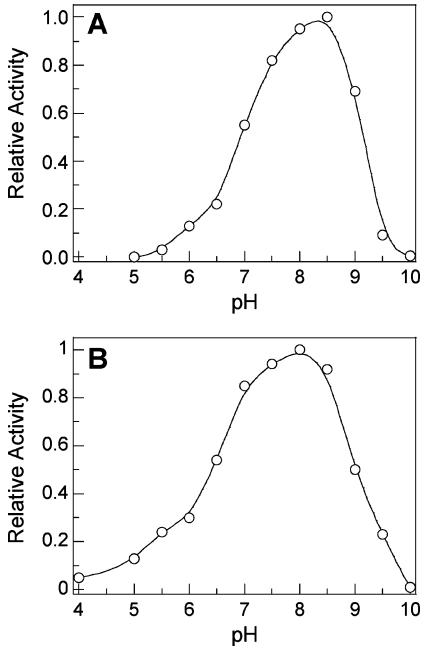

FIGURE 4: Effect of pH on the catalytic activity of fMAP (A) and fMDF (B).

Table 5: Kinetic Constants of fMAP toward *N*-formyl and *N*-acetyl Peptides

substrate	K_M (mM)	k_{cat} (s^{-1})	k_{cat}/K_M (M^{-1} s^{-1})
f-M-*p*NA	0.40 ± 0.20	46 ± 2	120000 ± 3000
	0.30 ± 0.15[a]	75 ± 4[a]	250000 ± 8500[a]
f-MLF	2.0 ± 0.8	4.6 ± 2.1	2300 ± 650
	0.60 ± 0.30[a]	14 ± 4[a]	22500 ± 2500[a]
	0.18[b]	12[b]	68000[b]
f-MF	0.60 ± 0.20	8.0 ± 3.3	13000 ± 4000
	0.5 ± 0.2[a]	51 ± 8[a]	101600 ± 9000[a]
	0.63[b]	70[b]	110000[b]
f-MA	0.5 ± 0.1	3.2 ± 0.9	6400 ± 640
f-MAS	2.3 ± 0.8	5.6 ± 2.1	2400 ± 500
f-MS	1.0	6.1	6100 ± 320
f-MSS	5.5 ± 2.0	4.2 ± 0.9	760 ± 180
f-MSSS	11 ± 3	4.0 ± 1.1	350 ± 130
f-MSSSS	12 ± 2	2.1 ± 1.3	180 ± 88
f-MSSSSS	30 ± 10	1.3 ± 1.2	43 ± 20
Ac-MAS	1.5 ± 0.3	4.4 ± 0.1	2930 ± 66
Ac-AA	1.0 ± 0.3	15 ± 4	15000 ± 3000
Ac-AAA	1.7 ± 0.4	13 ± 5	8000 ± 2000

[a] Values obtained at pH 8.0. [b] Literature values (from ref *15*).

tively (data not shown).

Catalytic Properties and Inhibition of fMAP (APH). To confirm the identity between fMAP and APH, the purified fMAP was examined for its pH dependence, substrate specificity, and sensitivity to effector molecules. With f-M-*p*NA as substrate, fMAP showed a bell-shaped pH profile with an optimal pH at 8.0−8.5 (Figure 4A), in excellent agreement with the results of Chadwick et al. (*15*) as well as the reported pH optimum of APH (*29*, *30*). fMAP is active toward both *N*-formyl- and *N*-acetyl peptides of two to six residues in length, but with the following trends (Table 5). First, fMAP strongly prefers a dipeptide substrate, showing progressively lower activities toward longer peptides (Table 5, compare f-MF vs f-MLF, f-MA vs f-MAS, f-MS vs f-MSS, and Ac-AA vs Ac-AAA). The increasing K_M values with peptide length suggest that fMAP binds dipeptides more effectively, perhaps by recognizing the α-carboxylate group of the penultimate residue. Second, the enzyme hydrolyzes

Table 6: Kinetic Properties of fMDF

substrate	K_m (mM)	k_{cat} (s^{-1})	k_{cat}/K_m ($M^{-1}s^{-1}$)
f-Met	3.1 ± 0.1	7.9 ± 0.1	2550 ± 77
	7.1[a]		
Ac-Met	0.3 ± 0.1	2.3 ± 0.9	7600 ± 500
	0.22[a]		
f-Met-Ala	NA	NA	NA
f-Ala-Ala	NA	NA	NA
f-Met-Ala-Ser	NA	NA	NA
Ac-Met-Ala-Ser	NA	NA	NA
f-Met-Leu-Phe	NA	NA	NA

NA = no activity detected. [a] Literature values (from ref *16*).

N-formyl and *N*-acetyl peptides with essentially equal efficiency (compare f-MAS and Ac-MAS). Finally, fMAP has a weak preference for a smaller amino acid at the N-terminus, showing ~2-fold higher activity toward *N*-alanyl peptides than *N*-methionyl peptides (compare f-MA and Ac-AA, Ac-MAS and Ac-AAA). Among all of the substrates tested, the artificial substrate, f-M-*p*NA (which mimics a dipeptide), is most active ($k_{cat}/K_m = 1.2 \times 10^5$ M^{-1} s^{-1} at pH 7.0). Importantly, fMAP efficiently hydrolyzes the chemotactic peptide f-MLF, with a k_{cat} value of 4.6 s^{-1}, a K_M value of 2.0 mM, and a k_{cat}/K_M value of 2300 M^{-1} s^{-1} (at pH 7.0). Thus, the catalytic properties and substrate specificity of our purified fMAP are in qualitative agreement with those reported for APH (*22*, *29*−*31*). Quantitative comparison was not possible as the literature values were relative activities determined at fixed substrate concentrations. To make proper comparisons of our results with those reported by Chadwick et al. (*15*), which were measured near its optimal pH (pH 8.0), we also determined the catalytic constants of fMAP toward f-M-*p*NA, f-MLP, and f-MF at pH 8.0 (Table 5). All three substrates exhibited higher activities than at pH 7.0 and the catalytic constants are in general agreement with those reported by Chadwick et al. (*15*).

Among the effector molecules tested, fMAP activity was not affected by the presence of 2-mercaptoethanol (5 mM), dithiothreitol (10 mM), or 100 μM divalent metal ions (Co^{2+}, Zn^{2+}, and Ni^{2+}). However, the enzyme was potently inhibited by diethyl pyrocarbonate (DEPC), which modifies histidine and cysteine residues in proteins (apparent IC_{50} = 35 nM). It is also inhibited by the serine protease inhibitor, phenylmethylsulfonyl fluoride (PMSF), with an apparent IC_{50} value of 150 μM. These results are in excellent agreement with those reported for fMAP by Chadwick et al. (*15*) and with the properties reported for APH, a member of the serine protease family (*22*, *29*−*31*). Further, both fMAP (*15*) and APH (*22*) are markedly inhibited or completely inactivated by Cu^{2+} and Hg^{2+} ions. Thus, all of our data support the hypothesis that fMAP and APH are the same enzyme.

Catalytic Properties and Inhibition of N-Acylase IA (fMDF). fMDF hydrolyzed both f-Met and Ac-Met to release free methionine, with slightly higher activity toward Ac-Met (k_{cat}/K_M of 7600 vs 2600 M^{-1} s^{-1}) (Table 6). Chadwick et al. reported the K_M values of 7.1 and 0.22 mM for f-Met and Ac-Met, respectively, at pH 8.0 (*16*). The optimal activity for fMDF is at pH 8.0 (Figure 4B), similar to that reported by Chadwick et al. (*16*). The corresponding values determined in this work (at pH 7.0) are 3.1 mM for f-Met and 0.3 mM for Ac-Met (Table 6). Comparison of k_{cat} values

was not possible because they were not reported by Chadwick et al. fMDF showed no activity against either N-formylated or N-acetylated di- and tripeptides (e.g., f-MA, f-AA, f-MAS, Ac-MAS, and f-MLF).

N-Acylase IA was previously reported as a zinc metalloenzyme, although the role of the metal ion in catalysis is still controversial (*32*, *33*). Atomic absorption studies of the purified fMDF sample revealed that the protein contains 0.98 Zn^{2+}/polypeptide. A metal content of 0.90 Zn^{2+}/polypeptide was also determined by a colorimetric assay using nitro-PAPS as the chromogenic ligand (*27*). To assess the possible role of the Zn^{2+} ion in catalysis, fMDF was assayed in the presence of effector molecules including various metal chelating agents. Preincubation with EDTA (50 mM) or 1,-10-phenanthroline (10 mM) resulted in 10% and 6% inhibition, respectively. Dithiothreitol (20 mM) and iodoacetamide (10 mM) produced stronger inhibition of 85% and 90%, respectively. N^{ϵ}-Formyl-N^{ϵ}-hydroxy-L-lysine, which contains a powerful bidentate metal ligand (*N*-formylhydroxylamine), inhibited fMDF with an IC_{50} value of 1.0 mM. Incubation of the enzyme with 100 μM $NiCl_2$ or $CoCl_2$ increased its catalytic activity by 2−3-fold. These results agree with those reported for fMDF by Chadwick et al. (*16*) and the properties of acylase IA (*34*, *35*). Further, stronger inhibition by smaller, bidentate metal ligands (e.g., dithiothreitol and N^{ϵ}-formyl-N^{ϵ}-hydroxy-L-lysine) than the bulkier multidentate ligands (e.g., EDTA) suggests that the Zn^{2+} is tightly bound to the protein, likely serving a catalytic role. Presumably, the smaller bidentate ligands can reach the active site and bind to the metal ion by replacing the metal-bound water, whereas EDTA and other bulky ligands inhibit the enzyme by removing the metal cofactor from the protein.

DISCUSSION

In this work, peptide mass fingerprinting has established that fMAP, as purified in this laboratory, is actually APH. We believe that Chadwick and co-workers (*15*) had previously purified the same enzyme as we did, based on the following reasons. First, both Chadwick et al. and we detected only one fraction that has detectable fMAP activity during purification. Both laboratories employed similar (though not identical) procedures to purify the enzyme. Second, the enzymes from the two laboratories share similar pH dependence, substrate specificities, and sensitivities to effector molecules. Several other observations also support the notion that Chadwick's fMAP is the same as APH. Chadwick et al. showed that their fMAP has a native M_r of 340 000 Da and a M_r 82 000 Da for each subunit (*15*), matching the molecular weights reported for full-length APH (*28*). APH and Chadwick's fMAP both have the same pH optimum (pH 7.9−9.0 for fMAP and pH 8.2 for APH) (*15*, *29*, *30*). Chadwick et al. reported that fMAP is broadly distributed in the body tissues including intestine, colons, rectum, kidney, and liver (*15*). The previously characterized rat APH was purified from liver tissues (*22*, *28*, *29*, *31*). The only inconsistency has been the difference in molecular mass of the purified enzymes; Chadwick et al. reported a M_r of 82 000, whereas our enzyme has a $M_r \sim 66\,000$ (Figure 3A). As mentioned above, our fMAP appears to be a proteolytic fragment of APH, although the precise location or mechanism of proteolytic cleavage of fMAP is presently unknown. It has previously been shown that APH contains a 55-kDa C-terminal peptide hydrolase domain and a 27-kDa N-terminal domain of unknown function (*32*−*34*). Limited proteolysis with trypsin separates the two domains at Arg193, Lys-195, or Lys196 positions, with little effect on its peptidase activity or in some cases slightly increased peptidase activities (*32*, *34*). We have noticed that a range of molecular masses have been reported for APH by previous investigators, including 80 kD (*31*), 75 kD (*22*, *34*), and 69 kD (*19*, *35*). N-Terminal sequencing of the 75 kD rat liver enzyme revealed an N-terminal glycine (*22*), whereas the N-terminal sequence of full-length APH should be Met-Glu-Arg-Gln-Val (*28*). When the porcine liver APH was overexpressed in *Escherichia coli*, the purified recombinant protein showed a major band at 69 kD and a minor band at ∼80 kD (*35*). All of the above observations suggest that the N-terminal region of APH (fMAP) is highly susceptible to proteolysis, and different purification procedures (e.g., the use of different protease inhibitors) likely have caused cleavage at different locations.

It appears that Chadwick and co-workers had concluded fMAP as an enzyme distinct from APH due to their less-than-optimal choice of assay substrates. These investigators examined the P_1 subsite specificity of their enzyme by testing against eight different formyl-amino acid-β-naphthylamide derivatives (*15*). They found that the enzyme was active only against the f-Met derivative but had no activity against the other derivatives (f-Ala, f-Val, f-Leu, f-Ser, f-Asp, f-Arg, or f-Phe-β-naphthylamides). All of the peptide substrates they tested contained an N-terminal methionine residue. These results led them to conclude that fMAP is "specific" for an N-terminal f-Met or acyl-Met moiety and thus distinct from APH, which has much broader substrate specificity (*22*, *28*, *29*, *31*).

fMDF activities have previously been described in the crude extracts of *Euglena gracilis* (*18*), rabbit reticulocyte lysates (*20*), human leukocytes and platelets (*17*), and a variety of other animal tissues (*36*). Chadwick et al. partially purified it from rat small intestines and examined its substrate specificity and sensitivity to a variety of effector molecules (*16*). However, the identity of fMDF has not been established. It was suggested by Grisolia et al. that fMDF might represent a previously unrecognized activity of acylase I (*36*). We have now shown that fMDF is indeed an acylase I variant. Acylases cleave *N*-acylamino acids into free amino acids and are thought to be important in the degradation of N-acylated peptides and proteins. In accordance with their substrate specificities, the acylases characterized so far can be classified into four different types, I−IV. Acylase I is responsible for the hydrolysis of neutral and hydrophobic *N*-acyl-L-amino acids. Two different forms of acylase I (IA and IB) have been found in rat kidney (*37*) and human liver (*38*), with 94% sequence identity between the two rat acylases. fMDF purified from rat intestinal mucosa corresponds to acylase IA. All of the peptides in Table 4 matched with tryptic fragments derived from acylase IA but not IB. Acylases IA and IB both contain 408 amino acids with a calculated molecular mass of ∼45 kDa (*37*, *38*). They have previously been shown as metalloproteins containing a single Zn^{2+} ion per polypeptide (*37*, *38*), in agreement with our metal analysis results. This explains why the activity of fMDF (acylase IA) is stimulated by divalent metal ions (Co^{2+} and Ni^{2+}) but inhibited by metal chelating agents. Previously,

the function of the metal ion has been a subject of debate (*39*, *40*). Our observation that small metal chelators strongly inhibit fMDF provides further evidence for a catalytic role for the metal ion.

Despite the broad distribution of APH and acylase I in animal tissues, their physiological functions have not been well understood other than their involvement in the degradation of *N*-acylated proteins. Our current work reveals an important second function for these enzymes, that is, degradation of N-formylated peptides. Indeed, both APH and acylase I hydrolyze N-formylated peptides with essentially the same efficiencies as their N-acetylated counterparts (Tables 5 and 6). Further, acylase I and APH genes in human and porcine have been mapped to chromosomes 3p21.1 and 3p21.3, respectively (*41*−*45*). The co-localization of these genes to the same chromosomal region suggests that these enzymes may be functionally linked in the sequential degradation of N-acylated peptides. By efficient degradation of chemotactic peptides such as f-MLF, APH and acylase I may provide the first line of defense against unwanted inflammatory responses at tissue sites that are in constant exposure to commensal bacteria (e.g., intestines). The abundance of these two enzymes coupled with their robust activities toward N-formylated peptides also suggests that treatment with PDF inhibitors is unlikely to induce inflammatory responses in a patient.

ACKNOWLEDGMENT

We thank Dr. Kari Green-Church and other staff at the Campus Chemical Instrument Center (The Ohio State University) for their assistance in the MS experiments.

REFERENCES

1. Meinnel, T., Mechulam, Y., and Blanquet, S. (1993) Methionine as translation start signal: a review of the enzymes of the pathway in *Escherichia coli*, *Biochimie 75*, 1061−1075.
2. Pei, D. (2001) Peptide deformylase: a target for novel antibiotics? *Emerging Ther. Targets 5*, 23−40.
3. Marasco, W. A., Phan, S. H., Krutzsch, H., Showell, H. J., Feltner, D. E., Nairn, R., Becker, E. L., and Ward, P. A. (1984) Purification and identification of formyl-methionyl-leucyl-phenylalanine as the major peptide neutrophil chemotactic factor produced by *Escherichia coli*, *J. Biol. Chem. 259*, 5430−5439.
4. Broom, M. F., Sherriff, R. M., Ferry, D. M., and Chadwick, V. S. (1993) Formylmethionyl-leucylphenylalanine and the SOS operon in *Escherichia coli*: a model of host-bacterial interactions, *Biochem. J. 291*, 895−900.
5. Nguyen, K. T., Hu, X., Colton, C., Chakratarti, R., Zhu, M. X., and Pei, D. (2003) Characterization of a human peptide deformylase: implications for antibacterial drug design, *Biochemistry 42*, 9952−9958.
6. Ye, R. D., and Boulay, F. (1997) Structure and function of leukocyte chemoattractant receptors, *Adv. Pharmacol. 39*, 221−289.
7. Schiffmann, E., Corcoran, B. A., and Wahl, S. M. (1975) *N*-formylmethionyl peptides as chemoattractants for leucocytes, *Proc. Natl. Acad. Sci. U.S.A. 72*, 1059−1062.
8. Schiffmann, E., Showell, H. V., Corcoran, B. A., Ward, P. A., Smith, E., and Becker, E. L. (1975) The isolation and partial characterization of neutrophil chemotactic factors from *Escherichia coli*, *J. Immunol. 114*, 1831−1837.
9. Carp, H. (1982) Mitochondrial *N*-formylmethionyl proteins as chemoattractants for neutrophils, *J. Exp. Med. 155*, 264−275.
10. Greaves, D. R., and Channon, D. M. (2002) Inflammation and immune responses in atherosclerosis, *Trends Immunol. 23*, 541−548.
11. Chadwick, V. S., Mellor, D. M., Myers, D. B., Selden, A. C., Keshavarzian, A., Broom, M. F., and Hobson, C. H. (1988) Production of peptides inducing chemotaxis and lysosomal enzyme release in human neutrophils by intestinal bacteria in vitro and in vivo, *Scand. J. Gastroenterol. 23*, 121−128.
12. Hobson, C. H., Roberts, E. C., Broom, M. F., Mellor, D. M., Sherriff, R. M., and Chadwick, V. S. (1990) Radio-immunoassay for formyl methionyl leucyl phenylalanine. I. Development and application to assessment of chemotactic peptide production by enteric bacteria, *J. Gastroenterol. Hepatol. 5*, 32−37.
13. Chester, J. F., Ross, J. S., Malt, R. A., and Weitzman, S. A. (1985) Acute colitis produced by chemotactic peptides in rats and mice, *Am. J. Pathol. 121*, 284−290.
14. Nast, C. C., and LeDuc, L. E. (1988) Chemotactic peptides. Mechanisms, functions, and possible role in inflammatory bowel disease, *Dig. Dis. Sci. 33*, 50S−57S.
15. Sherriff, R. M., Broom, M. F., and Chadwick, V. S. (1992) Isolation and purification of *N*-formylmethionine aminopeptidase from rat intestine, *Biochim. Biophys. Acta 1119*, 275−280.
16. Broom, M. F., Sherriff, R. M., Tate, W. P., Collings, J., and Chadwick, V. S. (1989) Partial purification and characterization of a formylmethionine deformylase from rat small intestine, *Biochem. J. 257*, 51−56.
17. Ackerman, S. K., and Douglas, S. D. (1979) *N*-Formyl-L-methionine deformylase activity in human leucocytes and platelets, *Biochem. J. 182*, 885−887.
18. Aronson, J. H., and Lugay, J. C. (1969) *N*-Formylmethionine deformylase from *Euglena gracilis*, *Biochem. Biophys. Res. Commun. 34*, 311−314.
19. Whitheiler, J., and Wilson, D. B. (1972) The purification and characterization of a novel peptidase from sheep red cells, *J. Biol. Chem. 247*, 2217−2221.
20. Yoshida, A., and Lin, M. (1972) NH_2-terminal formylmethionine- and NH_2-terminal methionine-cleaving enzymes in rabbits, *J. Biol. Chem. 247*, 952−957.
21. Jones, W. M., and Manning, J. M. (1988) Substrate specificity of an acylaminopeptidase that catalyzes the cleavage of the blocked amino termini of peptides, *Biochim. Biophys. Acta 953*, 357−360.
22. Tsunasawa, S., Narita, K, and Ogata, K. (1975) Purification and properties of acylamino acid-releasing enzyme from rat liver, *J. Biochem. 77*, 89−102.
23. Termignoni, C., Freitas, J. O., Jr., and Guimaraes, J. A. (1986) Removal of N-terminal methionine from hemoglobin nascent peptides by a membrane-bound rat liver methionine aminopeptidase, *Biochem. J. 234*, 469−473.
24. Kobayashi, K., and Smith, J. A. (1987) Acyl-peptide hydrolase from rat liver. Characterization of enzyme reaction, *J. Biol. Chem. 262*, 11435−11445.
25. Radhakrishna, G., and Wold, F. (1986) Purification and characterization of an *N*-acylaminoacyl-peptide hydrolase from rabbit muscle, *J. Biol. Chem. 261*, 9572−9575.
26. Fu, H., Dahlgren, C., and Bylund, J. (2003) Subinhibitory concentrations of the deformylase inhibitor actinonin increase bacterial release of neutrophil-activating peptides: a new approach to antimicrobial chemotherapy, *Antimicrob. Agents Chemother. 47*, 2545−2550.
27. Makino, T. (1990) A sensitive, direct colorimetric assay of serum zinc using nitro-PAPS and microwell plates, *Clin. Chim. Acta 197*, 209−220.
28. Kobayashi, K., Lin, L. W., Yeadon, J. E., Klickstein, L. B., and Smith, J. A. (1989) Cloning and sequence analysis of a rat liver cDNA encoding acyl-peptide hydrolase, *J. Biol. Chem. 264*, 8892−8899.
29. Gade, W., and Brown, J. L. (1978) Purification, characterization and possible function of alpha-*N*-acylamino acid hydrolase from bovine liver, *J. Biol. Chem. 253*, 5012−5018.
30. Unger, T., Nagelschmidt, M., and Struck, H. (1979) *N*-Acetylaminoacyl-*p*-nitranilidase from human placenta. Purification and some properties, *Eur. J. Biohem. 97*, 205−211.
31. Mitta, M., Miyagi, M., Kato, I., and Tsunasawa, S. (1998) Identification of the catalytic triad residues of porcine liver acylamino acid-releasing enzyme, *J. Biochem. 123*, 924−931.
32. Polgar, L., and Patthy, A. (1992) Cleavage of the Lys196−Ser197 bond of prolyl oligopeptidase: enhanced catalytic activity for one of the two resulting active enzyme forms, *Biochemistry 31*, 10769−10773.
33. Sharma, K. K., and Ortwerth, B. J. (1993) Bovine lens acylpeptide hydrolase. Purification and characterization of a tetrameric enzyme resistant to urea denaturation and proteolytic inactivation, *Eur. J. Biochem. 216*, 631−637.
34. Durand, A., Villard, C., Giardina, T., Perrier, J., Juge, N., and Puigserver, A. (2003) Structural properties of porcine intestine acylpeptide hydrolase, *J. Protein Chem. 22*, 183−191.

35. Senthilkumar, R., and Sharma, K. K. (2002) Effect of chaotropic agents on the structure−function of recombinant acylpeptide hydrolase, *J. Protein Chem. 21*, 323−332.
36. Grisolia, S., Reglero, A., and Rivas, J. (1977) *N*-Formyl-methionine deformylase of animal tissues, *Biochem. Biophys. Res. Commun. 77*, 237−244.
37. Perrier, J., Durand, A., Giardina, T., and Puigserver, A. (2004) The rat kidney acylase 1. Evidence for a new cDNA form and comparisons with the porcine intestinal enzyme, *Comp. Biochem. Physiol., Part B: Biochem. Mol. Biol. 138*, 277−283.
38. Schuchman, D. H., Jackson, C. E., and Desnick, R. J. (1990) Human arylsulfatase B: MOPAC cloning, nucleotide sequence of a full-length cDNA, and regions of amino acid identity with arylsulfatases A and C, *Genomics 6*, 149−154.
39. Heese, D., Berger, S., and Rohm, K. H. (1990) Nuclear magnetic relaxation studies of the role of the metal ion in Mn^{2+}-substituted aminoacylase I, *Eur. J. Biochem. 188*, 175−180.
40. Loffer, H. G., Kroll, M., and Scheneider, F. (1975) Inhibition of amino-acylase from hog kidney by 2-ethoxy-1-(ethoxycarbonyl)-1,2-(dihydroquinoline). *Biol. Chem. Hoppe−Seyler 368*, 481−485.
41. Cook, R. M., Burke, B. J., Buchhagen, D. L., Minna, J. D., and Miller, Y. E. (1993) Human aminoacylase-1. Cloning, sequence, and expression analysis of a chromosome 3p21 gene inactivated in small cell lung cancer, *J. Biol. Chem. 268*, 17010−17017.
42. Mitta, M., Ohnogi, H., Yamamoto, A., Kato, I., Sakiyama, F., and Tsunasawa, S. (1992) The primary structure of porcine aminoacylase I deduced from cDNA sequence, *J. Biochem. 112*, 737−742.
43. Miyagi, M., Sakiyama, F., Kato, I., and Tsunasawa, S. (1995) Complete covalent structure of porcine liver acylamino acid-releasing enzyme and identification of its active site serine residue, *J. Biochem. 118*, 771−779.
44. Erlandsson, R., Boldog, F., Persson, B., Zabarovsky, E. R., Allikmets, R. L., and Jornvall, H. (1991) The gene from the short arm of chromosome 3, at D3F15S2, frequently deleted in renal cell carcinoma, encodes acylpeptide hydrolase, *Oncogene 6*, 1293−1295.
45. Jones, W. M., Scaloni, A., Bossa, F., Popowicz, A., Schneewind, O., and Manning, J. M. (1991) Genetic relationship between acylpeptide hydrolase and acylase, two hydrolytic enzymes with similar binding but different catalytic specificities, *Proc. Natl. Sci. U.S.A. 88*, 2194−2198.

BI050191O